

Kinetics and mass transfer aspects about the adsorption of tartrazine by a porous chitosan sponge

Vanessa M. Esquerdo¹ · Thais M. Quintana¹ ·
Guilherme L. Dotto² · Luiz Antonio A. Pinto¹

Received: 19 March 2015 / Accepted: 3 June 2015 / Published online: 11 June 2015
© Akadémiai Kiadó, Budapest, Hungary 2015

Abstract Kinetic and mass transfer aspects about the adsorption of tartrazine on a porous chitosan sponge (PCS) were elucidated. PCS was prepared and characterized. The kinetic curves were obtained in batch mode at different stirring rates and initial dye concentrations. The kinetic data were evaluated by the pseudo-first order, pseudo-second order (PSO), Elovich and Avrami models. The mass transfer aspects were evaluated by the external mass transfer coefficient (k_f), intraparticle diffusion coefficient (D_{int}) and modified Biot number (B_i). The results revealed that PCS presented specific surface area around of $1150 \text{ m}^2 \text{ g}^{-1}$ and porosity of 92 %. The adsorption kinetics was favored at higher values of stirring rate and initial dye concentration. PSO and Elovich models were suitable to represent the kinetic data. The k_f values ranged from 7.38×10^{-3} to $5.25 \times 10^{-1} \text{ m s}^{-1}$ and the D_{int} values ranged from 8.93×10^{-10} to $4.72 \times 10^{-9} \text{ m}^2 \text{ s}^{-1}$. The B_i values at lowest stirring rates and initial dye concentrations showed that the external mass transfer should be considered. Otherwise, a complete dominance of intraparticle diffusion occurred at highest values of stirring rate and initial dye concentration.

Keywords Adsorption · Biot · Dyes · Kinetic · Porous structure · Tartrazine

List of symbols

a Initial velocity due to dq/dt with $q_t = 0$ ($\text{mg g}^{-1} \text{ min}^{-1}$)
ARE Average relative error (%)

✉ Guilherme L. Dotto
guilherme_dotto@yahoo.com.br

¹ Unit Operation Laboratory, School of Chemistry and Food, Federal University of Rio Grande, Rio Grande 96203–900, Brazil

² Environmental Processes Laboratory, Chemical Engineering Department, Federal University of Santa Maria (UFSM), 1000 Roraima Avenue, Santa Maria, RS 97105–900, Brazil

b	Desorption constant of the Elovich model (g mg^{-1})
B_i	Biot number (dimensionless)
C_0	Initial dye concentration (mg L^{-1})
C_t	Dye concentration at time t (mg L^{-1})
D_{int}	Intraparticle diffusion coefficient ($\text{m}^2 \text{s}^{-1}$)
f	Fitting parameter of Eq. (8) (dimensionless)
k_1	Rate constant of pseudo-first order model (min^{-1})
k_2	Rate constant of pseudo-second order model ($\text{g mg}^{-1} \text{min}^{-1}$)
k_{AV}	Avrami kinetic constant (min^{-1})
k_e	Late-stage adsorption rate constant (min^{-1})
k_f	External mass transfer coefficient (m s^{-1})
n	Fractional exponent of the Avrami model (dimensionless)
q_0	Concentration in the adsorbent in equilibrium with a liquid concentration (mg g^{-1})
q_1	Theoretical value of the adsorption capacity for the PFO model (mg g^{-1})
q_2	Theoretical value of the adsorption capacity for the PSO model (mg g^{-1})
q_{AV}	Theoretical value of the adsorption capacity for the Avrami model (mg g^{-1})
q_e	Experimental equilibrium adsorption capacity (mg g^{-1})
q_t	Amount of dye adsorbed at time t (mg g^{-1})
r_0	Initial adsorption rate ($\text{mg g}^{-1} \text{min}^{-1}$)
R	Adsorbent radius (m)
R^2	Coefficient of determination (dimensionless)
R_{adj}^2	Adjusted determination coefficient (dimensionless)
t	Time (min)
V	Volume of solution (L)
W	Adsorbent amount (g)

Greek symbols

α	Fitting parameter of Eq. (6) (min^{-1})
ρ_p	Adsorbent density (kg m^{-3})

Introduction

Dyes are important additives in food processing. These compounds are widely used, and the consumers tend to expect and accept its presence. However, during food processing, a considerable amount dye containing effluents is generated [1]. Furthermore, several azo dyes, such as tartrazine, have been reported to cause allergic reactions [2]. Thus, colored effluents should be carefully treated. These effluents are difficult to treat since the dyes are stable and have a synthetic origin and also a complex molecular structure [3]. Among the existing technologies, adsorption is an attractive way to remove dyes from aqueous effluents, because it is effective, environmentally and economically viable [4–6].

Chitosan is a biodegradable, non-toxic and hydrophilic biopolymer, which is obtained from the chitin deacetylation. It is recognized in the literature that the

adsorption onto chitosan is an emerging alternative technology to remove dyes from aqueous media [7, 8]. However, the majority of studies uses chitosan in powder form [5, 7, 9], but in this form, chitosan shows disadvantages, such as, low values of specific surface area and porosity [7]. Therefore, it is interesting to develop porous chitosan based materials for use as adsorbents. Recently, our research group developed a chitosan scaffold to remove five food dyes from aqueous media [10]. In this previous study, the equilibrium and thermodynamic data were evaluated. However, there is no available data in the literature regarding the kinetic and mass transfer aspects of tartrazine adsorption onto a porous chitosan sponge.

In solid/liquid homogeneous systems, the investigation of kinetic and mass transfer aspects is fundamental to determine the residence time, the factors affecting the operation and the rate controlling steps [5, 9, 11–14]. Generally, in the studies about dye removal on chitosan based materials, the kinetic investigation is based on the adsorption reaction models [5, 7, 9, 11]. These models provide a good representation of the experimental data and are simple from the mathematical viewpoint [11]. However, this work assumes that the adsorption kinetics can be represented in the same manner as the rate of a chemical reaction [11, 12]. Based on these models, it is not possible to obtain the mass transfer parameters and identify the rate controlling steps. On the other hand, the diffusional mass transfer models are constructed on the basis of three consecutive steps: external mass transfer, intraparticle diffusion and adsorption on active sites; and so represents more realistically the adsorption kinetics [15–17]. The use of both adsorption reaction models and diffusional models provides a good interpretation of the kinetic and mass transfer aspects in an adsorption process [5, 9, 11, 12, 16].

The objective of this study was to investigate the adsorption kinetics and mass transfer aspects of the system PCS-tartrazine. PCS was obtained and characterized by scanning electron microscopy (SEM), BET surface area and Fourier transform infrared spectroscopy (FT-IR). Adsorption kinetic curves were obtained at different stirring rates (50 and 150 rpm) and initial dye concentrations (50, 200 and 400 mg L⁻¹). The models of pseudo-first order (PFO), pseudo-second order (PSO), Elovich and Avrami were fitted with the experimental data. An alternative procedure was used for the estimation of external mass transfer coefficient (k_f), intraparticle diffusion coefficient (D_{int}) and modified Biot number (B_i).

Experimental

Adsorbate

The food azo dye tartrazine (FD&C Yellow 5, color index 19,140, molecular weight 534.4 g mol⁻¹, molecular size 18 Å and wavelength 425 nm) was used as adsorbate. The dye was supplied by Duas Rodas Ind (Brazil) and had purity higher than 85 %.

Preparation and characterization of porous chitosan structure

Chitosan powder (deacetylation degree of 85 ± 1 % and molecular weight of 147 ± 5 kDa) was obtained from shrimp wastes (*P. brasiliensis*) [18]. PCS was

prepared by dissolving 2 g of chitosan powder in 100 ml of 1 % (w/w) acid acetic solution. This solution was maintained under magnetic stirring for 24 h at room temperature, and then it was homogenized (Dremel, 1100–01, Brazil) for 5 min at 10,000 rpm. Subsequently, the solution was maintained at 193 K during 48 h in an ultrafreezer (Indrel, IULT 90–D, Brazil) and afterward, it was freeze dried (Liobras, 1108, Brazil) at 219 K for 48 h under vacuum of 44 mm Hg (Liobras, 1108, Brazil) [10].

The textural characteristics of PCS were observed by scanning electron microscopy (SEM) (Jeol, JSM–6060, Japan) [19]. The specific surface area and porosity were determined by a volumetric adsorption analyzer (Quantachrome instruments, New Win 2, USA) using the BET method [12]. The functional groups were identified by Fourier transform infrared spectroscopy (FT-IR) (Prestige, 21210045, Japan) [20].

Adsorption experiments

The adsorption experiments were carried out using solutions prepared from stock solutions of the dye tartrazine. The pH was adjusted to 6.0 by buffer disodium phosphate/citric acid solution (0.1 mol L^{-1}), which did not present interaction with the dye. The reagents used in the experimental assays were of analytical grade. Distilled water was used to prepare all solutions. The kinetic assays were carried out in a thermostated shaker (Innova 44, New Brunswick Scientific, USA) at different stirring rates (50 and 150 rpm) and different initial dye concentration (50, 200 and 400 mg L^{-1}) under the following fixed conditions: temperature of $298 \pm 1 \text{ K}$ and PCS concentration of 250 mg L^{-1} . Aliquots were taken at predetermined time intervals (from 0 to 630 min) and analyzed. The dye concentration was determined by spectrophotometry (Quimis, Q108 DRM, Brazil), and blanks were performed. All experiments were carried out in triplicate ($n = 3$). The amount of dye adsorbed at time t (q_t) was determined as [7]:

$$q_t = \frac{(C_0 - C_t)}{W} V \quad (1)$$

Here, C_0 , and C_t (mg L^{-1}) are the dye concentrations at $t = 0$ and at any time, respectively, W (g) is the adsorbent amount and V (L) is the volume of the solution.

Kinetic models

In order to verify the adsorption kinetic behavior, the pseudo-first order (PFO), pseudo-second order (PSO), Elovich and Avrami models were fitted with the experimental data.

The kinetic models of pseudo-first order (PFO) [21] and pseudo-second order (PSO) [22] are based in the adsorption capacity. The PFO model (Eq. 2) is generally applicable over the initial 20–30 min of the sorption process, while the PSO model (Eq. 3) is suitable for the whole range of contact time.

$$q_t = q_1(1 - \exp(-k_1t)) \quad (2)$$

$$q_t = \frac{t}{(1/k_2q_2^2) + (t/q_2)} \tag{3}$$

Here, k_1 and k_2 are the rate constants of pseudo-first order and pseudo-second order models, respectively in (min^{-1}) and ($\text{g mg}^{-1} \text{min}^{-1}$), q_1 and q_2 are the theoretical values for the adsorption capacity (mg g^{-1}).

The characteristic curve based on Elovich model (Eq. 4) is between those PFO model and intraparticle diffusion model [23].

$$q_t = \frac{1}{a} \ln(1 + abt) \tag{4}$$

being, ‘a’ is the initial velocity due to dq/dt with $q_t = 0$ ($\text{mg g}^{-1} \text{min}^{-1}$), ‘b’ is the desorption constant of the Elovich model (g mg^{-1}).

Avrami [24], proposed an alternative kinetic equation, based on the thermal decomposition, which has been used also for adsorption systems [9], as shown in Eq. 5:

$$q_t = q_{AV}(1 - \exp(-k_{AV}t)^n) \tag{5}$$

Here, k_{AV} is the Avrami kinetic constant (min^{-1}), q_{AV} is the theoretical Avrami adsorption capacity (mg g^{-1}), ‘n’ is a fractional exponent.

Mass transfer aspects

The mass transfer aspects of tartrazine adsorption on PCS were elucidated by the estimation of external mass transfer coefficient (k_f), intraparticle diffusion coefficient (D_{int}) and modified Biot number (B_i). These mass transfer parameters were estimated from the kinetic curves, using a new simplified method, which was proposed by Yao and Chen [25]. Based on Eq. 1 and the film surface diffusion model [12, 15], the early-stage kinetic equation was proposed as [25]:

$$q_t = \frac{r_0t}{1 + \alpha t} \tag{6}$$

Here, α is a fitting parameter (min^{-1}) and r_0 is the initial adsorption rate ($\text{mg g}^{-1} \text{min}^{-1}$), given by Eq. 7:

$$r_0 = \frac{3C_0k_f}{R\rho_p} \equiv \left(\frac{dq_t}{dt} \right)_{t=0} \tag{7}$$

Here, R is the adsorbent radius (m) and ρ_p is the adsorbent density (kg m^{-3}). According to Yao and Chen [25], the early-stage kinetic data, which corresponds to the range of the adsorbed amount (q_t) from zero to about half of the equilibrium value (q_e), can be fitted with Eq. 6, and then, the k_f values can be found by Eq. 7.

In the same way, the D_{int} values ($\text{m}^2 \text{s}^{-1}$) were estimated by fitting the late-stage kinetic data [which corresponds to the range of the adsorbed amount (q_t) from 70 to 100 % of the equilibrium value (q_e)] with the late-stage kinetic equation (Eq. 8):

$$\frac{q_t}{q_e} = 1 - \exp(-f - k_e t) \quad (8)$$

The late-stage kinetic equation was based on an approximation of Reichenberg equation used for Boyd plot at long adsorption times. In Eq. 8, ‘f’ is a fitting parameter and k_e (min^{-1}) is defined as the late-stage adsorption rate constant, given by Eq. 9:

$$k_e = \frac{D_{\text{int}} \pi^2}{R^2} \frac{1 + \frac{W}{V} \left(\frac{dq}{dc} \right)_e}{\frac{R^2}{D_{\text{int}} \pi^2} + \frac{R \rho_p}{3k_f} \left(\frac{dq}{dc} \right)_e} \quad (9)$$

To verify the predominance of intraparticle diffusion in relation to the external mass transfer, the modified Biot number (B_i) was calculated by Eq. 10 [15, 16]:

$$B_i = \frac{k_f R C_0}{q_0 \rho_p D_{\text{int}}} \quad (10)$$

Here, q_0 (mg g^{-1}) is the solid phase concentration in the adsorbent in equilibrium with a residual hypothetical liquid concentration.

Statistical evaluation of the fitted models

The kinetic and mass transfer parameters were determined by the fit of the models with the experimental data through nonlinear regression. The Simplex/Quasi-Newton estimation method was used and the calculations were performed through the Statistic software (Statistic 9.1, Statsoft, USA). The fit quality was measured by the coefficient of determination (R^2), adjusted determination coefficient (R_{adj}^2) and average relative error (ARE) [26].

Results and discussion

Main characteristics of PCS

Fig. 1 shows the SEM image of PCS. In this figure it can be observed that PCS presented a porous structure. This porous structure is important for adsorption purposes once it allows the access of the dye molecules into the internal sites [7, 10]. In addition, the specific surface area was around of $1150 \text{ m}^2 \text{ g}^{-1}$ and the porosity was 92 %. The literature presents values of specific surface area of $4.2 \text{ m}^2 \text{ g}^{-1}$ and porosity lower than 1 % for chitosan powder [27]. This shows that the preparation of PCS is efficient to improve the chitosan characteristics for adsorption purposes. The PCS radius (R) was 0.00125 m and ρ_p was 1550 kg m^{-3} . The large increases in specific surface area and porosity can be attributed to the preparation method as follows: under acid conditions the chitosan NH_3 groups are protonated, leading to the expansion of polymeric chains. Coupled to this, the intense agitation can provided more effective shocks between the polymeric chains,

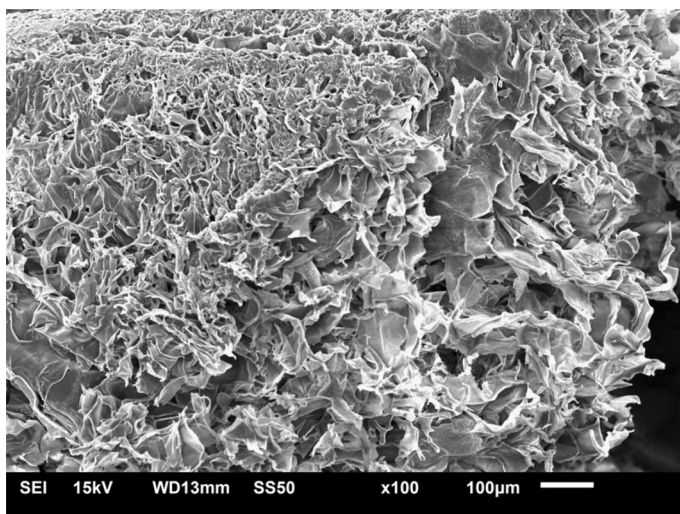


Fig. 1 SEM image of a porous chitosan structure ($\times 100$)

forming new links. These new links formed a porous structure. The solvent was removed by freeze dried, maintaining the structure.

The main functional groups of PCS were identified by FT-IR (Fig. 2). At 3200 cm^{-1} the broad band is relative to the O–H and N–H stretchings. At 1700 cm^{-1} can be observed the vibration of amide band I. The bands at 1550 and 1400 cm^{-1} can be assigned the C–N stretchings of amide and the angular deformation of C–O–H and H–C–H links, respectively. The band at 1000 cm^{-1} represents the C–O links, and the N–H links are shown at 680 cm^{-1} band. From the bands obtained on FT-IR, it can be affirmed that PCS presents the typical groups of chitosan (NH_2 and OH), which are potential sites for dyes adsorption [5, 7, 8, 10].

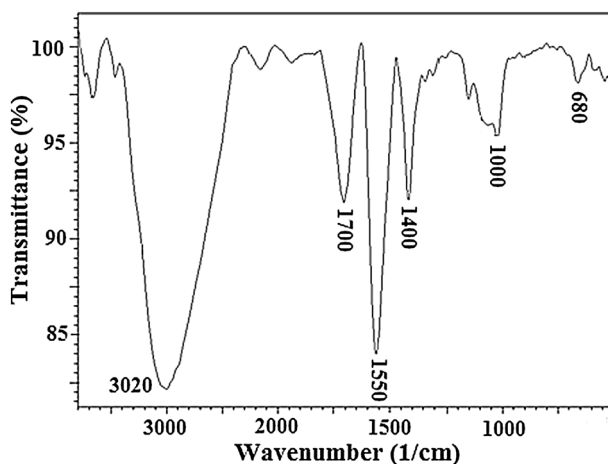


Fig. 2 FT-IR vibrational spectrum of a porous chitosan structure

Kinetic results

Fig. 3 shows the adsorption kinetic curves of tartrazine onto PCS at different initial dye concentrations (50, 200 and 400 mg L⁻¹) and stirring rates [(a) 50 and (b) 150 rpm]. The kinetic curves show that the adsorption capacity was enhanced when the stirring rate and initial dye concentration were increased. The adsorption equilibrium was faster attained at highest initial dye concentrations and stirring rates. The equilibrium adsorption capacities were 80.0, 202.0 and 373.7 mg g⁻¹ for

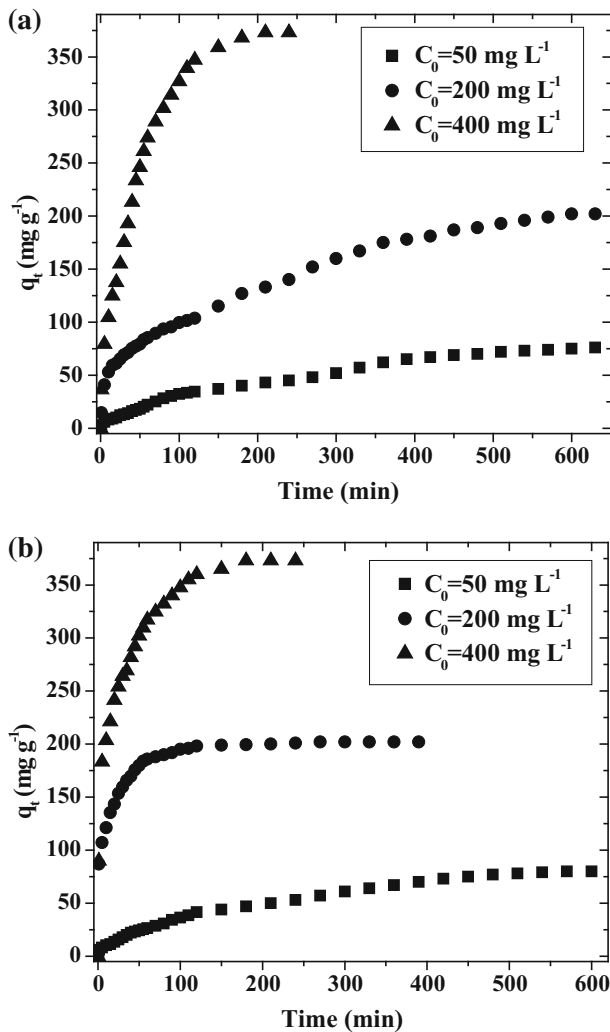


Fig. 3 Kinetic curves for the adsorption of tartrazine by PCS at different initial concentrations: **a** 50 rpm and **b** 150 rpm (filled square 50 mg L⁻¹, filled circle 200 mg L⁻¹, filled triangle 400 mg L⁻¹) (pH 6.0, temperature of 298 K, adsorbent dosage of 250 mg L⁻¹)

the initial dye concentrations of 50, 200 and 400 mg L⁻¹, respectively. The stirring rate effect can be explained by the highest power dissipation in the system at 150 rpm. This stirring rate increase also lead to a decrease in the external mass transfer resistance, facilitating the migration of the dye molecules to the PCS surface and, increasing the adsorption capacity in the early steps [5]. Dotto and Pinto [16] obtained similar results in the biosorption of synthetic dyes by *Spirulina platensis*. Regarding to the initial dye concentration, its increase provides the necessary driving force to overcome the resistance to the mass transfer of dye between the aqueous and the solid phases. Therefore, an increase in the initial concentration of dye enhances the adsorption capacity [14]. Chiou and Li [28], observed the effect of dye concentration on the adsorption kinetics of reactive red 189 by cross-linked chitosan, and found similar trend.

To investigate the tartrazine adsorption onto PCS, the experimental data were fitted with different kinetic models, like pseudo-first order (PFO), pseudo-second order (PSO), Elovich and Avrami. The kinetic parameters are shown in Table 1. Based on the high values of coefficient of determination ($R^2 > 0.92$), adjusted determination coefficient ($R_{adj}^2 > 0.91$) and in the low values of the average relative error (ARE < 14.0 %) presented in Table 1, it was found that the PSO and Elovich models were the most appropriate to represent the kinetic data of tartrazine adsorption by PCS. Table 1 shows that the parameters q_2 , k_2 , 'b', and 'ab' increased with initial dye concentration and stirring rate, confirming the experimental observations. The h_0 ($h_0 = k_2(q_2)^2$) parameter increased with initial dye concentration and stirring rate, indicating that, at the initial stages, the adsorption was faster at 400 mg L⁻¹ and 150 rpm.

Mass transfer results

The mass transfer aspects of tartrazine adsorption on PCS were elucidated by the estimation of external mass transfer coefficient (k_f), intraparticle diffusion coefficient (D_{int}) and modified Biot number (B_i). It was found that the early-stage kinetic equation (Eq. 6) fitted very well with the experimental data ($R^2 > 0.96$ and ARE < 10.0 %). In the same way, the late-stage kinetic equation (Eq. 8) fitted very well with the experimental data ($R^2 > 0.97$ and ARE < 7.0 %). This confirms the mass transfer steps (external mass transfer and intraparticle diffusion) and allows the accurate estimation of k_f , D_{int} and B_i . The results are shown in Table 2.

It was found in Table 2 that the external mass transfer coefficient (k_f) increased with the stirring rate and initial dye concentration. This shows that the transference of the tartrazine molecules from the bulk solution to the external surface of PCS was facilitated at highest values of stirring rate and initial dye concentration. The explanation for this behavior was presented in the above section (section Kinetic results). Similar behavior was found by Dotto et al. [15] in the adsorption of food dyes onto chitosan films. The D_{int} values ranged from 8.93×10^{-10} to 4.72×10^{-9} m² s⁻¹ and increased with the initial dye concentration. These values are high in relation to the following solid/liquid adsorption systems: chitin–tartrazine, chitosan–tartrazine [9], activated carbon–organic compounds [12], chitosan films–food dyes

Table 1 Kinetic parameters for the tartrazine adsorption on PCS

Dye initial concentration (mg L ⁻¹)	Stirring rate					
	50 rpm			150 rpm		
	50	200	400	50	200	400
PFO						
q ₁ (mg g ⁻¹)	77.5	185.2	370.4	78.7	192.0	341.2
k ₁ (min ⁻¹)	0.0046	0.0088	0.0223	0.0059	0.0872	0.0641
R ²	0.9797	0.8962	0.9858	0.9743	0.8381	0.8735
R ² _{adj}	0.9785	0.8904	0.9850	0.9728	0.8291	0.8664
ARE (%)	16.23	20.02	8.44	15.65	8.38	11.49
PSO						
q ₂ (mg g ⁻¹)	100.0	191.5	396.0	100.0	202.2	371.6
k ₂ × 10 ⁴ (g mg ⁻¹ min ⁻¹)	0.44	0.80	0.88	0.71	8.70	2.92
h ₀ (mg g ⁻¹ min ⁻¹)	0.44	2.935	13.80	0.71	35.57	40.32
R ²	0.9866	0.9220	0.9693	0.9642	0.9248	0.9501
R ² _{adj}	0.9858	0.9176	0.9675	0.9622	0.9206	0.9473
ARE (%)	11.28	13.21	9.62	11.92	6.35	7.09
Elovich						
a (mg g ⁻¹ min ⁻¹)	0.0317	0.0203	0.0090	0.0348	0.0456	0.0174
b (g mg ⁻¹)	0.5	4.1	17.4	0.7	1066.4	209.5
ab (min ⁻¹)	0.0162	0.0839	0.1568	0.0258	48.679	3.6404
R ²	0.9919	0.9701	0.9821	0.9932	0.9658	0.9931
R ² _{adj}	0.9914	0.9684	0.9811	0.9928	0.9639	0.9927
ARE (%)	9.47	9.89	7.78	8.39	4.17	2.28
Avrami						
n	0.298	0.222	0.1053	0.3144	0.558	0.243
q _{av} (mg g ⁻¹)	77.5	185.2	370.4	78.7	192.0	341.2
k _{av} (min ⁻¹)	0.0155	0.0400	0.0212	0.0190	0.1563	0.2639
R ²	0.9797	0.8962	0.9859	0.9743	0.8381	0.8735
R ² _{adj}	0.9785	0.8904	0.9851	0.9728	0.8291	0.8664
ARE (%)	15.81	19.49	8.02	16.08	7.95	11.45

PFO pseudo-first order, *PSO* pseudo-second order

Table 2 Mass transfer parameters for the tartrazine adsorption on PCS

Stirring rate (rpm)	C ₀ (mg L ⁻¹)	Q _c (mg g ⁻¹)	K _f × 10 ³ (m s ⁻¹)	D _{int} × 10 ⁹ (m ² s ⁻¹)	B _i
50	50	80.0	7.38	0.89	4.2
50	200	202.0	27.5	1.11	19.7
50	400	373.7	30.8	3.31	8.0
150	50	80.0	10.8	1.36	4.0
150	200	202.0	449.0	4.56	78.6
150	400	373.7	525.0	4.72	95.9

[15], *Spirulina*–synthetic dyes [16], Chitosan–FD&C red 40 [27] and others [25]. This probably is a result of the PCS characteristics, which is composed for larger porous, facilitating the mass transfer inside the particles. From the B_i values (Table 2), it was found that at lowest stirring rates and initial dye concentrations, the external mass transfer should be considered ($B_i < 10$). On the other hand, a complete dominance of intraparticle diffusion occurred at highest values of stirring rate and initial dye concentration.

SEM images

The SEM images of PCS before and after the adsorption of tartrazine are presented in Fig. 4. PCS presented porous network before the adsorption process (Fig. 4a). However, these textural characteristics were modified after adsorption (Fig. 4b).

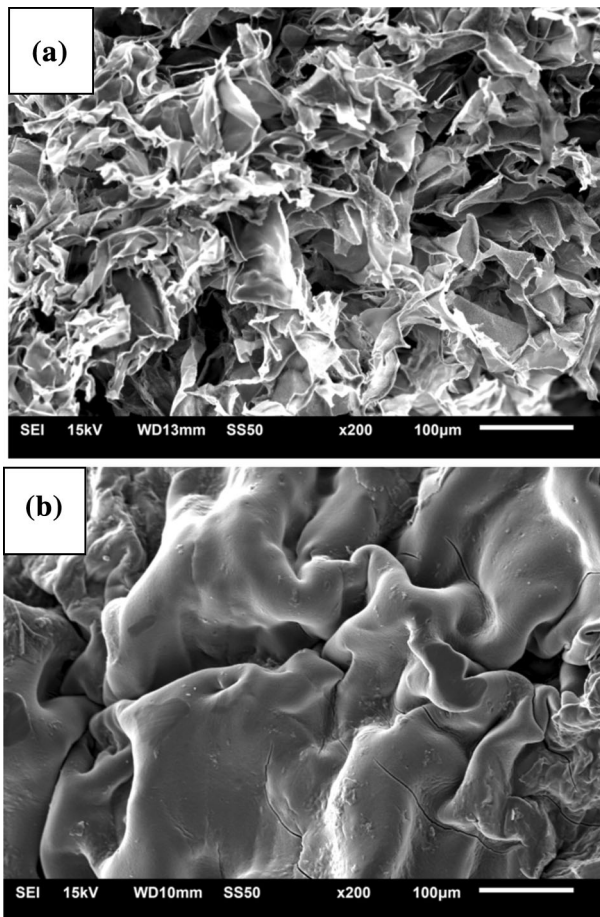


Fig. 4 SEM images of chitosan scaffold ($\times 200$): **a** before adsorption process and **b** after adsorption process

Table 3 Comparison between PCS and other adsorbents used to remove tartrazine from aqueous solutions

Adsorbent	pH	T (K)	Adsorption capacity (mg g ⁻¹)	Reference
PCS	6.0	298	373.7	This work
Papaya seeds	2.5	298	51.0	[29]
Chitin powder	3.0	298	30	[9]
Chitosan powder	3.0	298	350	[9]
Magnetic chitosan	3.0	298	292.07	[30]
Activated carbon	2.0	323	90.9	[31]
Hen feather	2.0	323	64.1	[32]
Chitosan–bentonite	2.5	318	294.1	[33]

The pores were filled and the surface was smoothed. This occurred due to the filling pores by water and dye molecules. These results confirm that the tartrazine were densely and homogeneously adhered onto the adsorbent.

Comparison with other adsorbents

In order to verify the efficiency of PCS, the adsorption capacity of PCS was compared with other adsorbents used for tartrazine removal. These results are shown in Table 3. It can be observed in Table 3 that PCS presented higher adsorption capacities than all adsorbents, including activated carbon. Another important fact is that the high adsorption capacity was attained at pH of 6.0. According to Hessel et al. [34] the pH of colored effluents is in the range from 5.5 to 8.5. This high adsorption capacity probably occurred due the high porosity and surface area of PCS.

Conclusion

In this work, the kinetic and mass transfer aspects about the tartrazine adsorption on a porous chitosan sponge (PCS) were studied. The results revealed that the adsorption was favored at highest stirring rates and initial dye concentrations. The PSO and Elovich models were the most suitable to represent the experimental kinetic curves. The k_f values ranged from 7.38×10^{-3} to 5.25×10^{-1} m s⁻¹ and the D_{int} values ranged from 8.93×10^{-10} to 4.72×10^{-9} m² s⁻¹.

The external resistance should be considered at lowest values of stirring rate and initial dye concentration. However, at the highest values of stirring rate and initial dye concentration, a complete dominance of intraparticle diffusion occurred. The SEM images showed that tartrazine was densely and homogeneously adhered to the PCS adsorbent. The adsorption capacity was 373.7 mg g⁻¹ at pH of 6.0, 298 K, 150 rpm and 400 mg L⁻¹ of dye. PCS presented higher adsorption capacity than other adsorbents shown in literature for the tartrazine removal.

Acknowledgments The authors would like to thank CAPES (Coordination for the Improvement of Higher Education Personnel) and CNPq (National Council for Scientific and Technological Development) for the financial support. Furthermore, the authors would like to thank CEME–SUL/FURG (Electron Microscopy Center of South/Federal University of Rio Grande/RS/Brazil) due to the scanning electron microscopy images.

References

1. Yagu MT, Sen TK, Afroze S, Ang HM (2014) *Adv Colloid Interface Sci* 209:172–184
2. Kobylewski S, Jacobson MF (2010) *Food dyes a rainbow of risks*. Center for Science in the Public Interest, Washington
3. Dotto GL, Pinto LAA, Hachicha MA, Knani S (2015) *Food Chem* 171:1–7
4. Gupta VK, Suhas (2009) *J Environ Manag* 90:2313–2342
5. Dotto GL, Pinto LAA (2011) *J Hazard Mater* 187:164–170
6. Ali I, Asim M, Khan TA (2012) *J Environ Manag* 113:170–183
7. Crini G, Badot PM (2008) *Prog Polym Sci* 33:399–447
8. Vakili M, Rafatullah M, Salamatinia B, Abdullah AZ, Ibrahim MH, Tan KB, Gholami Z, Amouzgar P (2014) *Carbohydr Polym* 113:115–130
9. Dotto GL, Vieira MLG, Pinto LAA (2012) *Ind Eng Chem Res* 51:6862–6868
10. Esquerdo VM, Cadaval TR, Dotto GL, Pinto LAA (2014) *J Colloid Interface Sci* 424:7–11
11. Qiu H, Pan LL, Zhang QJ, Zhang W, Zhang Q (2009) *J Zhejiang Univ Sci A* 10:716–724
12. Leyva-Ramos R, Ocampo-Perez R, Mendoza-Barron J (2012) *Chem Eng J* 183:141–151
13. Wu JT, Kuo CY, Wu CH (2015) *Reac Kinet Mech Cat* 114:341–355
14. Haji S, Khalaf M, Shukrallah M, Abdullah J, Ahmed S (2015) *Reac Kinet Mech Cat* 114:795–815
15. Dotto GL, Buriol C, Pinto LAA (2014) *Chem Eng Res Des* 92:2324–2332
16. Dotto GL, Pinto LAA (2012) *Biochem Eng J* 68:85–90
17. Ruthven DM (1984) *Principles of Adsorption and Adsorption Processes*. Wiley, New York
18. Dotto GL, Souza VC, Pinto LAA (2011) *LWT Food Sci Technol* 44:1786–1792
19. Goldstein JI, Newbury DE, Echil P, Joy DC, Romig AD, Lyman CE (1992) *Scanning electron microscopy and X-Ray microanalysis*. Plenum Press, New York
20. Silverstein RM, Webster FX, Kiemle DJ (2007) *Spectrometric identification of organic compounds*. Wiley, New York
21. Lagergren S (1898) *Kung Sven Vetensk Hand* 24:1–39
22. Ho YS, McKay G (1998) *Process Saf Environ Prot* 76B:332–340
23. Wu FC, Tseng RL, Juang RS (2009) *Chem Eng J* 150:366–373
24. Avrami M (1939) *J Chem Phys* 7:1103–1112
25. Yao C, Chen T (2015) *Chem Eng J* 265:93–99
26. El-Khaiary MI, Malash GF (2011) *Hydrometallurgy* 105:314–320
27. Piccin JS, Dotto GL, Vieira MLG, Pinto LAA (2011) *J Chem Eng Data* 56:3759–3765
28. Chiou MS, Li HY (2002) *J Hazard Mater B* 93:233–248
29. Weber CT, Collazzo GC, Mazutti MA, Foletto EL, Dotto GL (2014) *Water Sci Technol* 70:102–107
30. Zhou Z, Lin S, Yue T, Lee TC (2014) *J Food Eng* 126:133–141
31. Gautam RK, Gautam PK, Banerjee S, Rawat V, Soni S, Sharma SK, Chattopadhyaya MC (2015) *J Environ Chem Eng* 3:79–88
32. Mittal A, Kurup L, Mittal J (2007) *J Hazard Mater* 146:243–248
33. Ngah WSW, Ariff NFM, Hanafiah MAKM (2010) *Water Air Soil Pollut* 206:225–236
34. Hessel C, Allegre C, Maisseu M, Charbit F, Moulin P (2007) *J Environ Manag* 83:171–180